Available online at www.sciencedirect.com
SCIENCE DIRECT®
Biochemical Pharmacology 66 (2003) 1151–1162
Biochemical Pharmacology
www.elsevier.com/locate/biochempharm

Taxol- and okadaic acid-induced destabilization of *bcl-2* mRNA is associated with decreased binding of proteins to a *bcl-2* instability element

Sumita Bandyopadhyay[a], Tapas K. Sengupta[a], Daniel J. Fernandes[a], Eleanor K. Spicer[a,b,*]

[a]*Department of Biochemistry and Molecular Biology, Medical University of South Carolina, 173 Ashley Avenue, P.O. Box 250509, Charleston, SC 29425, USA*
[b]*Department of Pharmaceutical Sciences, Medical University of South Carolina, 173 Ashley Avenue, P.O. Box 250509, Charleston, SC 29425, USA*

Received 22 January 2003; accepted 1 June 2003

Abstract

The observation that overexpression of the anti-apoptotic protein Bcl-2 is associated with both cancer development and anti-cancer drug resistance suggests that factors which regulate *bcl-2* expression may be important therapeutic targets. We report here that taxol or okadaic acid (OA) treatment of HL-60 cells reduced *bcl-2* mRNA steady state levels to 50% of control cell levels in 20–24 hr of treatment. The 3′-untranslated region of *bcl-2* mRNA contains four potential A + U-rich elements (AREs), which are associated with mRNA destabilization. RNA gel mobility shift assays revealed that HL-60 cell extracts contain proteins that bind to RNA transcripts containing the first *bcl-2* ARE (ARE 1). ARE 1 binding activity was substantially reduced in extracts of cells treated for 20 hr with taxol or OA and was abolished after 32 hr of treatment. UV-induced RNA cross-linking assays revealed that untreated HL-60 cell extracts contain approximately eight proteins, ranging in size from 32 to 100 kDa, that bind to ARE 1 RNA. Following 20 hr of taxol or OA treatment, RNA cross-linking to ~70 and ~38 kDa proteins was greatly reduced, and cross-linking to four proteins of 45–60 kDa sizes was progressively reduced with 10–34 hr of OA or taxol treatment. Collectively, these results suggest a novel action of taxol and OA on *bcl-2* expression, which involves *bcl-2* mRNA downregulation through inactivation of *bcl-2* mRNA stabilizing factors.

Keywords: *Bcl-2* gene expression; mRNA stability; Taxol; Okadaic acid; mRNA instability element; Leukemia

1. Introduction

Bcl-2 was one of the first proto-oncogenes that was observed to promote carcinogenesis by prolonging cell survival rather than increasing cell replication [1]. Overexpression of Bcl-2 is thought to be an important component in the development of B-cell lymphomas that contain a t(14;18) translocation, which moves the *bcl-2* gene into the IgH locus near a transcriptional enhancer [2]. Overexpression of *bcl-2* also is seen in other cancers where translocation and enhanced transcription of *bcl-2* has not occurred [3]. Moreover, high Bcl-2 expression in some malignant cells is an obstacle to chemotherapeutic treatment, since it interferes with drug-induced apoptosis [4–6]. Accordingly, factors that regulate the expression of *bcl-2* may be important therapeutic targets for reversing both the malignant phenotype and anti-cancer drug resistance.

While inhibitors of Bcl-2 protein function have been studied extensively, comparatively little is known about factors that regulate *bcl-2* transcription or mRNA stability. Previous studies have shown, however, that taxol-induced apoptosis of OV2008 ovarian cancer cells is associated with downregulation of *bcl-2* mRNA as well as Bcl-2 protein [7]. Subsequently, Riordan *et al.* [8] found that apoptosis of

* Corresponding author. Tel.: +1-843-792-7475; fax: +1-843-792-8565.
E-mail address: spicerek@musc.edu (E.K. Spicer).

Abbreviations: UTR, untranslated region; ARE, A + U-rich element; OA, okadaic acid; taxol, paclitaxel; CAT, chloramphenicol acetyl transferase; RT–PCR, reverse transcription–polymerase chain reaction; GST-HuR, glutathione-S-transferase-HuR fusion protein; FITC, fluorescein isothiocyanate; PBS, phosphate-buffered saline; AEBSF, 4-(2-aminoethyl)benzenesulfonyl fluoride; DMEM, Dulbecco's modified Eagle's medium; PVDF, polyvinylidene fluoride; TBE, Tris–borate–EDTA; TAE, Tris–acetate–EDTA.

0006-2952/$ – see front matter © 2003 Elsevier Inc. All rights reserved.
doi:10.1016/S0006-2952(03)00453-2

HL-60 cells induced by OA is preceded by decreases in *bcl-2* mRNA and protein levels, while actin and Bcl-X_L protein levels are unaffected. Interestingly, both Liu and Priest [7] and Riordan *et al.* [8] found that decreased *bcl-2* mRNA levels were due to mRNA destabilization rather than decreased transcription. This is an interesting observation since it suggests that *trans*-acting factors that regulate the stability of *bcl-2* mRNA can play an important role in the response of cancer cells to apoptotic stimuli.

Cis-elements that regulate mRNA stability have been identified in numerous cytokine [9,10] and oncogene [11,12] mRNAs. Prominent among these is the ARE that is found in the 3′-UTR of mRNAs that have short half lives [13]. Although there is little sequence similarity between AREs, they typically contain multiple copies of an AUUUA pentamer within an A + U-rich region. AREs have been divided into three classes, based upon their sequence features and the kinetics of mRNA decay [14]. The 3′-UTR of *bcl-2* mRNA contains a conserved ARE [15] that has the features of a Class I ARE [14]. The *bcl-2* ARE consists of a A + U-rich region containing two pentamers and a cluster of three overlapping pentamers. Similar to the Class I AREs found in c-*fos* [16] and c-*myc* [17] mRNAs, the *bcl-2* ARE can confer instability on an intrinsically stable mRNA in transfected cells [15]. The observation that a reporter-*bcl-2–ARE* fusion mRNA was further destabilized by treatment of transfected cells with C_2-ceramide suggests that the ARE may play a role in the regulation of *bcl-2* expression by apoptotic agents [15]. Donnini *et al.* [18] subsequently reported that multiple proteins in Jurkat cell extracts bind to the *bcl-2* ARE *in vitro* and that the pattern of ARE-binding proteins changes following treatment of cells with UV-C irradiation. Recently, it was reported [19] that the ARE-binding protein AUF1 binds to the *bcl-2* ARE *in vitro* and *in vivo*. It was further found that UV-C irradiation of Jurkat cells was associated with increased complex formation between a *bcl-2* ARE riboprobe and the p45 isoform of AUF1 present in cell extracts, suggesting that AUF1 plays a role in UV-C-induced downregulation of *bcl-2* mRNA.

Since induction of DNA damage by UV-C treatment may produce different effects on *bcl-2* mRNA regulating factors than those induced by taxol or OA, it remains unclear how taxol or OA modulate *bcl-2* mRNA stability. In particular, it is not known if taxol produces similar affects on *bcl-2* mRNA and its regulating factors as OA. Also, it is not clear whether taxol- or OA-induced *bcl-2* mRNA downregulation involves inactivation of *bcl-2* mRNA stabilizing factors such as HuR or activation of destabilizing factors such as AUF1. To address these questions, we have examined the effects of taxol and OA on *bcl-2* mRNA stability in HL-60 cells, where the level of *bcl-2* mRNA is elevated relative to normal B cells and Jurkat T cells [20]. RNA gel mobility shift assays were employed to probe for proteins that bind to the first of the four potential AREs in *bcl-2* mRNA. Additionally, we have examined the effects of taxol and OA on ARE-binding proteins in HL-60 cells to better understand the relationship between *trans*-acting factors and *bcl-2* mRNA stability in specific cancer cells.

2. Materials and methods

2.1. Cell culture

Human HL-60 leukemia cells (ATCC) were grown in RPMI-1640 medium (Gibco-BRL), supplemented with 10% (v/v) fetal bovine serum (Gibco-BRL), 100 U/mL penicillin and 100 μg/mL streptomycin, at 37° in 5% CO_2. Mouse NIH 3T3 cells (ATCC) were grown in DMEM (American Type Culture Collection) with 10% fetal bovine serum (Atlanta Biologicals), 2 mM glutamine, 50 U/mL of penicillin and 50 μg/mL of streptomycin at 37° in 5% CO_2.

2.2. Taxol and OA treatment of HL-60 cells

Cells (2×10^6) were transferred to 10 mL fresh medium and then grown for 2 hr before addition of either 20 nM OA (Sigma Chemical Co.) or 200 nM taxol (Sigma). To determine *bcl-2* mRNA half-life, cells were treated with taxol or OA for 25 hr and then 1 μg/mL actinomycin D (Sigma) was added to the medium. At various time points, cells were harvested, washed with PBS, resuspended in RLT buffer (Qiagen Inc.) and stored at −70°, for subsequent RNA isolation.

2.3. RNA isolation and RT–PCR

Total cellular RNA was isolated from 2×10^6 HL-60 cells using an RNeasy™ kit (Qiagen Inc.). Equal amounts of total RNA from treated or untreated cells were reverse transcribed using MMLV reverse transcriptase (Promega Inc.) and random hexamers. PCR amplifications of the cDNAs were carried out with primer pairs for the *bcl-2* gene (5′-GGAAGTGAACATTTCGGTGAC-3′ and 5′-GCCTCTCCTCACGTTCCC-3′) and *β-actin* gene (5′-GCGGGAAATCGTGCGTGACAT-3′ and 5′-GATGGAGTTGAAGGTAGTTTC-3′) using Taq DNA polymerase (Promega). Samples were incubated for 1 min at 94°, 1 min at 57° and 1 min at 72°, for 26 cycles for *bcl-2* or for 24 cycles for *β-actin* amplification, followed by incubation at 72° for 7 min. PCR products were analyzed on a 2% agarose gel, stained with SYBER Green-I™ (Molecular Probes, Inc.) and the band intensities were quantitated using a STORM™ phosphorimager and Image QuaNT™ software (Molecular Dynamics).

2.4. Flow cytometric analysis of drug-induced apoptosis in HL-60 cells

HL-60 cells (2×10^6) in 10 mL RPMI medium were treated with 20 nM OA or 200 nM taxol for 0–45 hr. After

treatment, 5×10^5 cells were removed and centrifuged at 100 *g* for 5 min at room temperature. Cell pellets were resuspended in 500 μL 1× binding buffer (Annexin V-FITC Apoptosis Detection Kit: Biovision) at room temperature. Five microliters FITC-labeled annexin V and 2.5 μL propidium iodide were added to each sample and reactions were incubated at room temperature in the dark for 5 min. Binding of annexin V to phosphatidylserine that has translocated to the external surface of the plasma membrane indicate cells in the early stages of apoptosis. Propidium iodide fluorescence distinguishes between necrotic cells (permeable to propidium iodide) and early apoptotic cells, which remain impermeable to propidium iodide. The percentages of viable, apoptotic and necrotic cells were determined in each sample using a FACSCalibur™ flow cytometer (Becton Dickinson).

2.5. Plasmid construction

ARE cDNA vectors for *in vitro* RNA transcription were prepared by RT–PCR cloning. For ARE 1, a 406 bp fragment corresponding to nucleotides # 745–1150 of *bcl-2* mRNA (GenBank accession # NM 000633 [2,21]) was prepared. ARE 1-A vectors contain a 137 bp fragment corresponding to nucleotides # 921–1057 of *bcl-2* mRNA. Total RNA prepared from 2×10^5 Jurkat cells was used as a template for cDNA synthesis using MMLV reverse transcriptase and random hexamers. The following pairs of PCR primers were used to amplify *bcl-2* ARE cDNAs—ARE 1: forward, 5′-CAAGTGAAGTCAACATGCCTGC-3′; reverse, 5′-GATGGTGATCCGGCCAACAAC-3′; ARE 1-A: forward, 5′-CAGTCTTCAGGCAAAACGTCGA-3′; reverse, 5′-GTGGTCGGATTTCCAAAGACA-3′. PCR products were purified from a 2% agarose gel and cloned into the pCR4-TOPO TA vector (Invitrogen) to produce plasmids pCR4-ARE-1 and pCR4-ARE-1-A. Plasmids were sequenced by automated DNA sequencing in the MUSC Biotechnology Resource Laboratory.

Plasmids pBBB4 and pBBB$^{c\text{-}fos}$ [16,22] containing the rabbit *β-globin* gene or the *β-globin-ARE*$^{c\text{-}fos}$ gene under the control of the serum-inducible c-*fos* promotor were a gift from Dr. A.-B. Shyu. Vectors containing *bcl-2* AREs inserted downstream from the *β-globin* gene on pBBB4 were constructed as follows: The vector specific primer pair forward: 5′-GCCGAGATCTGGTTTAAACGAATT-CGGCC-3′ and reverse: 5′-GCGCAGATCTGCGGCCG-CGAATTCGCCC-3′ containing *Bgl*II restriction sites (underlined) was used to PCR-amplify ARE 1-A and ARE 1 from pCR4-ARE-1-A and pCR4-ARE-1 plasmids, respectively. The 197 and 466 bp PCR products were digested with *Bgl*II, gel purified, and cloned into the *Bgl*II site of pBBB4 plasmid to produce pBBB-ARE$^{bcl\text{-}1\text{-}A}$ and pBBB-ARE$^{bcl\text{-}1}$, respectively. Plasmids for preparation of *β-globin* and *CAT* antisense probes for RNase protection assays were constructed as follows: plasmid pBBB4 and primer pair forward: 5′-CTGCTGGTCGTCTACCCTTG-GAC-3′ and reverse: 5′-CTCACTCAGTGTGGCAAAGG-TG-3′ were used to amplify 180 bp of the *β-globin* coding region, which was then cloned into the pCR4-TOPO vector, to produce pCR4-β-globin. Plasmid pCAT (Promega) and primer pair 5′-GGACTTTCCACACCTGGTTGCTG-3′ and 5′-GCACCTGTCCTACGAGTTGCATG-3′ were used to amplify 234 bp of the bacterial *CAT* gene, which was then cloned into pCR4.

2.6. Preparation of RNA transcripts

ARE transcripts were synthesized using T7 RNA polymerase from *Spe*I-linearized plasmids pCR4-ARE-1 and pCR4-ARE-1-A. Antisense *β-globin* and *CAT* mRNA transcripts were synthesized from *Spe*I-linearized plasmids pCR4-*β-globin* and pCR4-*CAT* where *β-globin* and *CAT* genes were in antisense orientation with respect to the T7 promoter. ^{32}P-labeled transcripts were synthesized using 0.5 μg linearized plasmid, 10 mM DTT, 500 μM each ATP, CTP and GTP, 250 μM UTP, 20 μCi ^{32}P-UTP (Pharmacia Amersham Biotech) and 40 units of T7 RNA polymerase in optimized transcription buffer (Promega). The purity of RNA transcripts was monitored by analysis on 6% polyacrylamide/7 M urea gels (Novex), and the amount of full length product was generally ≥90% of the total.

2.7. Transient transfections and RNase protection assays

NIH 3T3 cells at ∼60% confluence were grown in DMEM medium in 60 mm dishes for 18 hr prior to transfection. Transfection was performed using Lipofectamine Plus™ reagent (Gibco-BRL) according to the manufacturer's directions. Cells were mixed with 2–3 μg of pBBB4 plasmids and 1 μg of control *pCAT* plasmid. After DNA addition, cells were grown for 16–18 hr and then serum-starved in DMEM/0.5% fetal bovine serum for 24 hr. Cells were then stimulated with DMEM/15% fetal bovine serum for 0–8 hr. After harvesting cells, total RNA was isolated using an RNeasy kit (Qiagen). *β-Globin* and *CAT* mRNA levels were measured by RNase protection assays using a Hybspeed RPA™ kit (Ambion). Equal amounts of RNA (10–20 μg) were combined with ^{32}P-labeled antisense *β-globin* (244 nt) and antisense *CAT* (298 nt) probes and the RNA/probe mixture was heated at 95° for 10 min, then incubated at 68° for 10 min. Samples were then digested with RNase A (5 units/mL) and T1 (20 units/mL) at 37° for 30 min. The samples were electrophoresed in a 6% polyacrylamide/TBE-7 M urea gel, which was fixed with 10% acetic acid and dried. Protected fragments were quantitated by phosphorimaging.

2.8. Preparation of HL-60 cell extracts

Cells (2×10^6) were centrifuged at 100 *g* for 5 min and the cell pellets were washed twice with PBS and then

stored at −80°. At the time of analysis, cell pellets were suspended in 200 μL buffer A (50 mM Tris–HCl, pH 7.5, 150 mM NaCl, protease inhibitor cocktail (Sigma) and 1 mM AEBSF (Sigma)). Cell suspensions were then sonicated on ice with three 10 s bursts using a Virsonic sonicator (Virtis) at a setting of 4. Sonicated cells were then centrifuged at 13,000 rpm in a microcentrifuge (Eppendorf) for 30 min. Supernatants were stored at 4° for a maximum of 7 days without loss of RNA binding activity. Protein concentrations were determined by absorbance at 280 nm.

2.9. In vitro mRNA decay assays

5′-Capped ^{32}P-labeled *bcl-2* ARE 1-A and *CAT* transcripts were prepared using a mMESSAGE mMACHINE T7 kit (Ambion), using *Spe*I linearized pCR4-ARE-1-A and pCR4-CAT plasmids, respectively. Poly(A) tails of approximately 150 nucleotides were added to the 3′-ends of the transcripts using a poly(A) tailing kit (Ambion). After poly(A) addition, unincorporated NTPs were removed by G-25 spin column chromatography. Approximately 150,000 cpm of capped and polyadenylated ARE or CAT mRNAs were used per reaction. Following the protocol of Ford and Wilusz [23], 14.25 μL decay assays contained 3.25 μL of 10% polyvinyl alcohol, 1 μL of a 12.5 mM ATP/250 mM phosphocreatine mixture, 1 μL 500 ng/μL poly(A) (Amersham Pharmacia Biotech), 1 μL ^{32}P-labeled transcript (50 nM), and 10 μg of HL-60 S100 extract. Reactions were incubated at 30° and aliquots were removed at various times and added to 100 μL of stop buffer (400 mM NaCl, 25 mM Tris–HCl, pH 7.5, 0.1% SDS), and immediately extracted with 100 μL of phenol–chloroform. RNA in the aqueous phase was ethanol precipitated in the presence of 0.5 M ammonium acetate and 15 μg yeast tRNA. Precipitated RNA samples were analyzed on 6% polyacrylamide gels containing 7 M urea. After electrophoresis, gels were fixed, dried and analyzed by phosphorimaging.

2.10. Expression and purification of recombinant HuR

Plasmid pGEX-HuR [24] containing the recombinant *GST-HuR* gene was a gift from Dr. Henry Furneaux. *E. coli* BL21 cells transformed with pGEX-HuR were grown overnight and then diluted 1:50 in LB medium and induced for 2 hr at 37° with 1 mM isopropylthiogalactoside. Following induction, cells were centrifuged, resuspended in 20 mL of buffer B (50 mM Tris–HCl, pH 8.0, 200 mM NaCl, 1 mM EDTA) and lysed by sonication. The lysate was centrifuged at 12,000 *g* for 30 min and the supernatant was applied to a 1 mL glutathione-agarose column (Amersham Pharmacia Biotech) equilibrated with buffer B. After washing with buffer B, GST-HuR was eluted with 50 mM Tris–HCl, pH 8.0, containing 5 mM glutathione. Protein purity was assessed by SDS–PAGE and protein concentration was measured spectrophotometrically at 280 nm.

2.11. RNA gel mobility shift assays

Cell extracts (7.5 μg of total protein) and ^{32}P-RNA transcripts (20,000 cpm) in 20 μL RNA binding buffer (50 mM Tris–HCl, pH 7.5, 150 mM NaCl, 0.025 mg/mL tRNA, 0.25 mg/mL bovine serum albumin) were incubated on ice for 10 min. Five microliters of gel loading solution (50% glycerol, 0.1% bromophenol blue, 0.1% xylene–cyanol) was then added to the reaction, and 10 μL of each sample were analyzed on a 1% agarose/TAE gel. To test for HuR binding, 5 μL GST-HuR (1.8 μg) was mixed with ^{32}P-ARE-1-A RNA in 20 μL binding buffer. For supershift assays, 20 μg/mL of monoclonal anti-HuR antibody (Molecular Probes) was added to the reaction mixture, which was incubated at room temperature for 10 min before addition of dye mixture and gel electrophoresis. For competition assays, 1× or 10× concentrations of competitor RNA (unlabeled ARE 1-A transcript) or non-competitor RNA (180 nucleotide β-globin coding region transcript) were added to the reaction before addition of total cell lysate. For all retardation assays, gels were dried on nitrocellulose paper and analyzed by phosphorimaging.

In combined gel retardation/Western blot assays, ^{32}P-ARE-1-A RNA was incubated in 10 μL binding buffer with 3.75–7.5 μg HL-60 cell extract protein or 0.15 μg GST-HuR protein on ice for 10 min. Complexes were digested with RNase T1 (5 units) at room temperature for 10 min and then electrophoresed on a 6% polyacrylamide retardation gel (Novex, Inc.). The gel was exposed to a phosphorimage plate for 30 min and then electro-transferred to PVDF membrane. The blot was probed with anti-HuR monoclonal antibody (Molecular Probes, Inc.) and developed with chemiluminescent Luminol Reagent (Santa Cruz Biotechnology).

2.12. UV-induced protein–RNA cross-linking

Five microliters of ^{32}P-ARE-1 RNA transcript (2×10^5 cpm) were incubated with 10 μL of HL-60 cell extracts (50 μg of total protein) in 1× RNA binding buffer on ice for 10 min. Reaction mixtures were then transferred to a 96 well microtiter plate on ice and exposed to 254 nm UV irradiation using a mineral light lamp (model UVG-54, Ultraviolet, Inc.) at a distance of 7 cm for 30 min. Following UV cross-linking, samples were digested with RNase A (0.01 units/μL) and RNase T1 (0.4 units/μL) at 37° for 30 min. Proteins were analyzed on a 12% polyacrylamide-SDS gel, which was stained with Coomassie Brilliant Blue R-250 (Bio-Rad), destained, and dried. Protein bands containing crosslinked RNA were identified by phosphorimaging of the dried gels.

3. Results

3.1. Taxol or OA treatment of HL-60 cells induces bcl-2 mRNA destabilization

Earlier studies indicated that OA treatment of HL-60 cells leads to decreased *bcl-2* mRNA half-life and induction of apoptosis [8]. To determine whether taxol treatment has a similar effect on *bcl-2* mRNA levels in HL-60 cells, steady state levels of *bcl-2* and *β-actin* mRNAs were measured as a function of taxol treatment for 0–32 hr. As shown in Fig 1A, semi-quantitative RT–PCR assays indicated that *bcl-2* mRNA steady state levels fell to ∼50% of control cell levels following 20 hr of treatment with 200 nM taxol. OA treatment decreased the steady state level of *bcl-2* mRNA in a similar time-frame, reducing it to ∼50% of control levels in ∼24 hr. The decay of *bcl-2* mRNA following addition of actinomycin D to HL-60 cultures was then monitored to determine whether the reduction in *bcl-2* mRNA steady state levels induced by taxol or OA is due to decreased stability of *bcl-2* mRNA. As shown in Fig. 1B, the half-life of *bcl-2* mRNA was reduced from ∼8.8 to ∼3.3 hr in cells treated with taxol for 25 hr and to 3.2 hr in OA-treated cells. Thus, the decrease in steady state levels of *bcl-2* mRNA is due, at least in part, to accelerated decay of *bcl-2* mRNA.

We considered the possibility that the observed reductions in *bcl-2* mRNA levels may be a secondary effect of the induction of apoptosis by the drug treatment. Therefore, we examined the time course of induction of apoptosis to see if *bcl-2* mRNA levels decrease before or after apoptosis is induced. The fraction of apoptotic cells present in HL-60 cultures was measured following treatment with taxol or OA for a period of 0–45 hr. Viable, apoptotic and necrotic HL-60 cells were identified by staining with FITC-labeled annexin V and propidium iodide followed by flow cytometric analysis [25]. The results of this analysis are shown in Fig. 1C, where the percentage of annexin V-positive (apoptotic) cells is plotted versus time after taxol or OA treatment. With taxol treatment, *bcl-2* mRNA levels were reduced to ≤50% within 20 hr (Fig. 1A), while ∼50% of cells had entered the early stage of apoptosis after 35 hr (Fig. 1C). A similar effect was seen with OA treatment where *bcl-2* mRNA was reduced to ≤50% within 24 hr, while 50% of the cells entered apoptosis after ∼35 hr of treatment. Neither taxol nor OA increased the number of necrotic (propidium iodide positive) cells

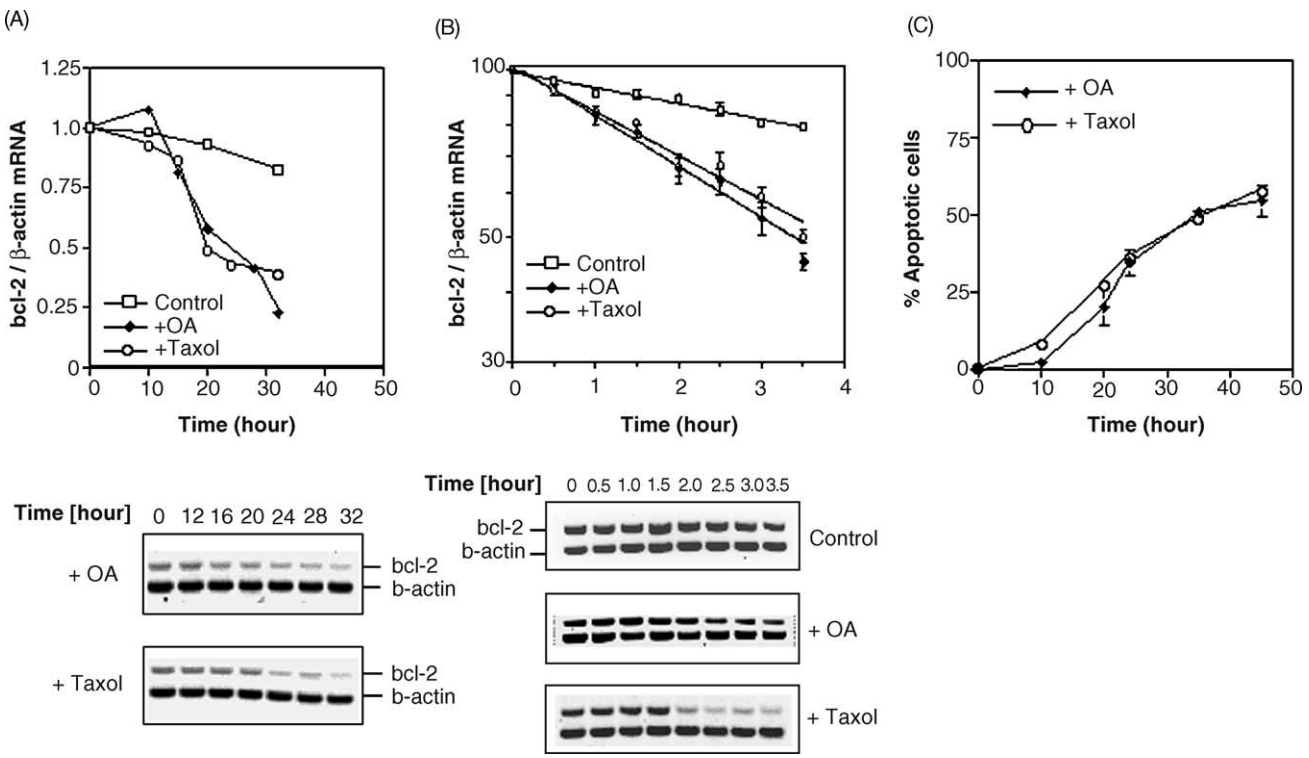

Fig. 1. Effect of taxol and OA on *bcl-2* mRNA steady state levels, *bcl-2* mRNA half-life, and induction of apoptosis in HL-60 cells. Cells were treated with taxol (200 nM) or OA (20 nM) for the times indicated. (A) Total RNA was extracted and steady state levels of *bcl-2* and *β-actin* mRNAs were determined by semi-quantitative RT–PCR. Values are the mean of *bcl-2*/*β-actin* mRNA ratios from three experiments. The variability at each time point was ≤5% relative to the maximal value. A representative RT–PCR analysis is shown below the graph. (B) Semilog plot showing decay of *bcl-2* mRNA. HL-60 cells were treated with taxol or OA for 25 hr and then actinomycin D was added for a period of 0–3.5 hr. Transcript levels were measured by quantitation of RT–PCR products and the amount of *bcl-2* mRNA was normalized to the amount of *β-actin* mRNA and plotted by linear regression. Values are the mean of *bcl-2*/*β-actin* ratios from three experiments. A representative RT–PCR analysis is shown below the graph. (C) Time course of induction of apoptosis. HL-60 cells were treated with taxol or OA and then incubated with FITC-labeled annexin V and propidium iodide. The percentage of viable (non-labeled) and apoptotic (annexin V-labeled) cells were counted by flow cytometry. The percentage of apoptotic cells is plotted versus length of taxol or OA treatment. Values are the average of two independent experiments. Error bars are shown for cells treated with taxol; similar variability was observed with OA-treated cells.

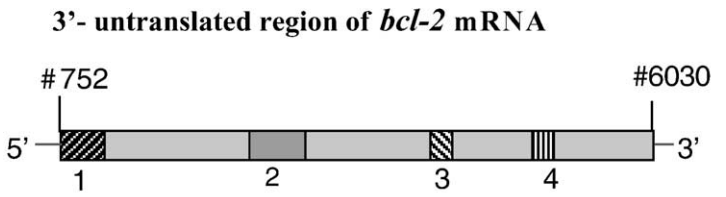

ARE 1	#752 - 1150	2 pentamers & $(AUU)_3A$
ARE 1-A	#921 - 1057	2 pentamers & $(AUU)_3A$
ARE 2	#2401 - 2940	3 pentamers
ARE 3	#4021 - 4260	2 pentamers
ARE 4	#4921 - 5161	2 pentamers & 1 hexamer

Fig. 2. Location of potential AREs in the 3′-UTR of *bcl-2* mRNA. Each of the indicated regions, containing two or more AUUUA pentamers within an A + U-rich sequence, is a potential Class I ARE [14]. Nucleotide #752 is the first nucleotide following the *bcl-2* coding region stop codon [2].

within this time frame (data not shown). Thus, downregulation of *bcl-2* mRNA in HL-60 cells treated with either taxol or OA appears to precede, rather than follow, the induction of apoptosis. The observation that *β-actin* mRNA levels were not significantly reduced following 32 hr of taxol or OA treatment (Fig. 1A) further supports the conclusion that *bcl-2* mRNA downregulation is not a secondary effect of the induction of apoptosis by drug treatment.

3.2. Bcl-2 mRNA contains four potential Class I AREs

Schiavone *et al.* [15] reported that *bcl-2* mRNA contains a functional ARE in the 3′-UTR. Inspection of the 5280-nucleotide-long 3′-UTR of *bcl-2* mRNA [2] using the program BLAST [26] reveals that there are three additional regions that are potential Class I AREs. These AREs, shown schematically in Fig. 2, each contain two to three AUUUA pentamers within an A + U-rich region. ARE IV also contains a hexamer (AUUUUA) that has been associated with mRNA instability [27]. In addition, ARE 1 (described by Schiavone *et al.* [15]) has three overlapping pentamers ($(AUUU)_3A$) which contain the nonamer sequence (UUAUUUAUU) that can trigger rapid deadenylation and decay when inserted into *β-globin* mRNA [28]. Within the 405 nucleotide ARE 1, there is a sequence of 137 nucleotides (referred to here as ARE 1-A) that

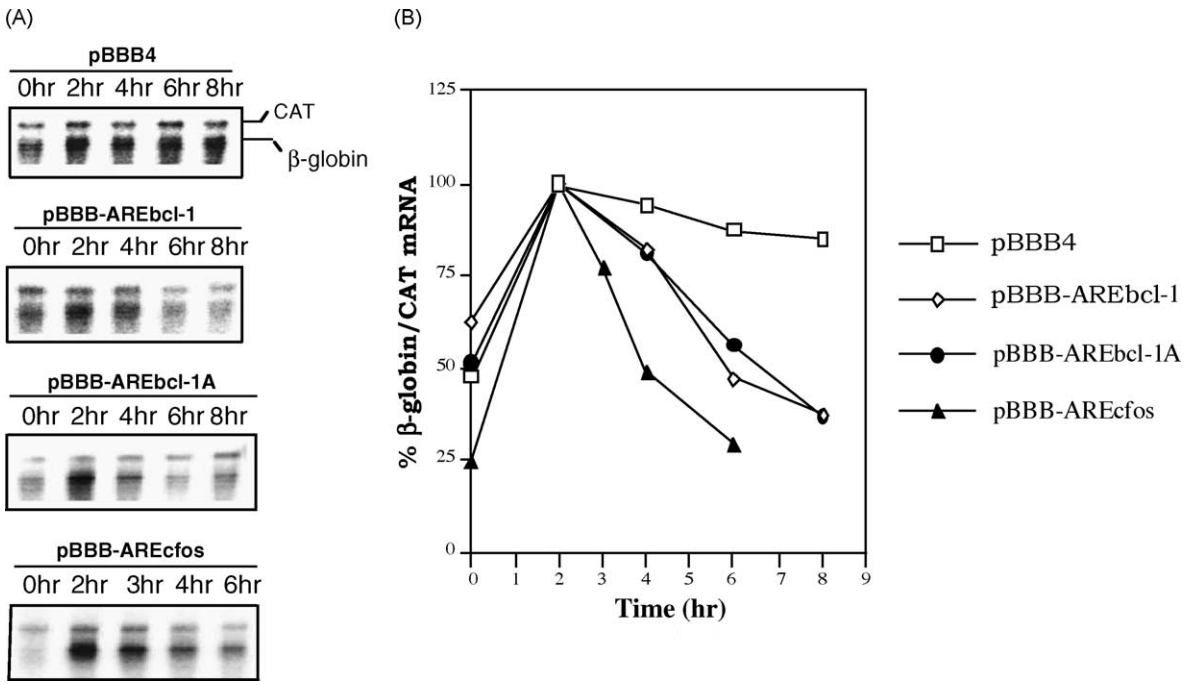

Fig. 3. Effect of *bcl-2* ARE-I on *β-globin* mRNA stability. *β-Globin* reporter plasmids were transiently co-transfected with *pCAT* vectors into NIH 3T3 cells. After 24 hr of serum starvation, *β-globin* transcription was stimulated by addition of fetal bovine serum. Cells were harvested at times shown. Total RNA was extracted and analyzed by RNase protection assays using antisense CAT and *β-globin* transcripts as probes. (A) Representative phosphorimage of RNase protection assays. (B) Plot of *β-globin* mRNA determined by phosphorimaging and normalized to *CAT* mRNA. Values are the mean of three experiments. The variability at each time point was ≤5% relative to the maximum signal which was set at 100% for each vector.

contains the two pentamers and the $(AUUU)_3A$ sequence, which is likely to be the functional part of ARE 1.

To compare the functional activities of ARE 1 and the smaller ARE 1-A, we performed transient transfection assays using a reporter *β-globin* gene. *Bcl-2* ARE 1 and ARE 1-A were cloned into plasmid pBBB4 [16,22] to generate pBBB-ARE^{bcl-1} and pBBB-ARE$^{bcl-1-A}$. In these vectors the AREs were inserted into the 3′-UTR of the *β-globin* gene which is downstream from the serum inducible c-*fos* promoter. Plasmids pBBB-ARE^{bcl-1} and pBBB-ARE$^{bcl-1-A}$ were each co-transfected into NIH 3T3 cells with a control plasmid pCAT, which constitutively expresses *CAT* mRNA. For reference, a positive control plasmid containing the strongly destabilizing c-*fos* ARE [22,29], pBBB-ARE^{c-fos}, and the parental pBBB4 plasmid lacking an ARE were co-transfected with pCAT into NIH 3T3 cells. Following 24 hr of serum starvation, cells were incubated in serum-rich medium to induce a burst of transcription from the c-*fos* promoter. To follow mRNA decay, cells were collected at 2 hr intervals for 0–8 hr after serum stimulation. Total RNA was extracted from harvested cells and the amount of *β-globin* and *CAT* mRNA in the RNA extracts was determined by ribonuclease protection assays. The levels of *β-globin* mRNA, normalized to the *CAT* mRNA, are shown in Fig. 3. For each vector, the maximum signal was taken as 100%. As expected, pBBB-ARE^{c-fos} mRNA decayed rapidly, falling to a level of ∼25% within 6 hr. The pBBB-ARE^{bcl-1} mRNA level also decreased more rapidly than the control pBBB4 mRNA levels, confirming that ARE 1 functions as an instability element when transfected into NIH 3T3 cells. The level of *β-globin ARE 1-A* mRNA decreased at a rate similar to that of *β-globin ARE-1*, suggesting that the entire destabilizing element is contained within the 137 nucleotides of ARE 1-A.

To test the hypothesis that taxol- and OA-induced *bcl-2* mRNA downregulation involves the ARE 1-A *cis*-element, the stability of a transcript containing ARE 1-A in HL-60 cells extracts was measured using the *in vitro* mRNA decay assay developed by Ford and Wilusz [23]. 5′-Capped, polyadenylated RNA transcripts carrying ARE 1-A (*bcl-2* ARE mRNA) or without an ARE (CAT mRNA) were incubated with S100 extracts of untreated or drug-treated HL-60 cells. At various times, the reactions were stopped and the abundance of the RNA was determined by gel electrophoresis. As shown in Fig. 4, *bcl-2* ARE mRNA decayed faster in taxol-treated ($T_{1/2}$ = 34 min) and OA-treated ($T_{1/2}$ = 38 min) cell extracts than in untreated cell extracts ($T_{1/2}$ = 76 min). In contrast, *CAT* mRNA exhibited similar decay rates in extracts of untreated ($T_{1/2}$ = 47 min) or drug-treated cells ($T_{1/2}$ = 42−47 min). Thus, taxol and OA treatment led to accelerated decay of ARE mRNA but not *CAT* mRNA. The fact that ARE 1-A RNA exhibited a longer half-life than *CAT* mRNA in extracts of untreated cells (Fig. 4) is consistent with the concept that HL-60 cells contain *bcl-2* ARE-specific stabilizing *trans*-acting factors.

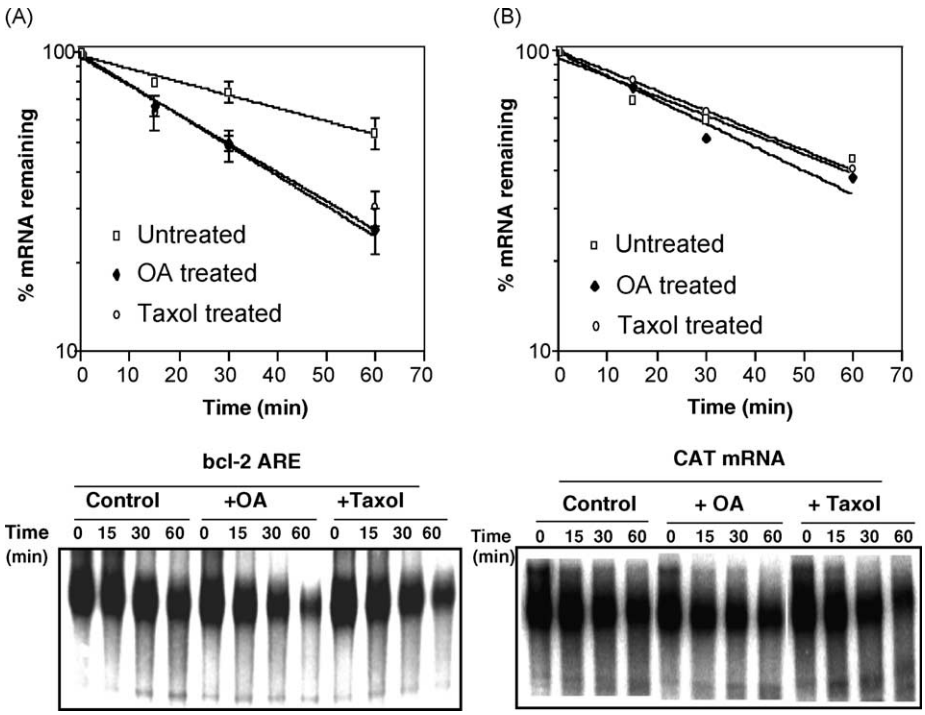

Fig. 4. Decay of *bcl-2* ARE 1-A mRNA in drug-treated and untreated HL-60 extracts. Semi-log plot showing the decay of ARE 1-A and CAT mRNAs in cell extracts. 5′-Capped, polyadenylated ^{32}P-labeled mRNAs were incubated with S100 extracts and aliquots were taken at various times. RNA recovery was assessed by electrophoresis on 5% polyacrylamide 7 M urea gels, which were analyzed by phosphorimaging. (A) Comparison of the decay of ARE mRNA in extracts of untreated and taxol- or OA-treated HL-60 cells. (B) Decay of CAT mRNA in extracts of drug-treated or untreated HL-60 cells. S100 extracts were prepared from untreated cells or cells treated for 20 hr with taxol (200 nM) or OA (20 nM). Data are the average from two (B) or three experiments (A).

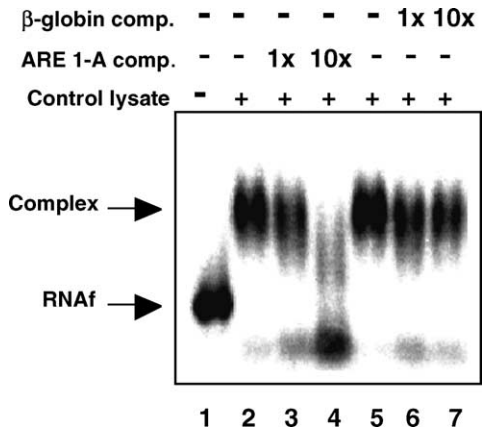

Fig. 5. HL-60 cell extracts contain *bcl-2* ARE 1-A binding proteins. A 200 nucleotide ^{32}P-labeled transcript containing *bcl-2* ARE 1-A was incubated with HL-60 cell extracts in the absence (lanes 2 and 5) or presence of 1- or 10-fold excess of unlabeled ARE 1-A (lanes 3 and 4) or *β-globin* (lanes 6 and 7) RNAs in binding buffer. Free and complexed RNAs were separated by electrophoresis on 1% agarose gels, which were analyzed by phosphorimaging.

3.3. HL-60 cells contain proteins that bind to bcl-2 ARE 1-A RNA

The observed destabilization of *bcl-2* mRNA following taxol or OA treatment of HL-60 cells (Fig. 1B) could be due to inactivation of a *bcl-2* mRNA stabilizing factor or due to activation of a destabilizing factor, such as an endonuclease, or to a combination of both processes. As a first step in probing for factors that interact with the *bcl-2* ARE in HL-60 cells, *in vitro* synthesized ARE 1-A RNA transcripts were tested for protein binding in RNA gel mobility shift assays. ^{32}P-labeled ARE 1-A transcripts were incubated with HL-60 cell extracts and the reactants were separated by gel electrophoresis. As shown in Fig. 5, incubation of ARE 1-A RNA (containing the 137 nucleotide ARE 1-A and 64 nucleotides of vector sequence) with HL-60 cell extracts produced a shift in the mobility of the RNA (lanes 2 and 5). The specificity of ARE binding was assessed by performing competition binding assays in the presence of a 1× or 10× concentration of unlabeled transcripts (in addition to a ≥1000× molar ratio of tRNA). As expected, addition of a 10-fold excess of unlabeled ARE 1-A RNA reduced the amount of ^{32}P-RNA–protein complex formed (Fig. 5, lane 4). In contrast, addition of a 10-fold excess of a non-ARE, *β-globin* transcript (lane 7) did not significantly decrease the amount of complex formed. It should be noted that in the presence of excess unlabeled ARE 1-A RNA, the electrophoretic mobility of the probe RNA was increased (Fig. 5). Analysis of the binding reaction on a denaturing gel indicated that ≥90% of the 200 nucleotide probe was full length. Thus, the altered migration of unbound probe is not due to nuclease digestion, but rather may reflect a change in the conformation of the RNA in the presence of cell extracts. These competition assays indicated that proteins present in the *bcl-2* ARE complexes have a ≥10-fold preference for *bcl-2* ARE RNA over *β-globin* mRNA and a ≥1000-fold preference over non-cognate tRNA.

3.4. Okadaic acid and taxol reduce the activity of bcl-2 ARE binding proteins in HL-60 cells

Further experiments were performed to determine whether the *bcl-2* ARE-binding proteins in HL-60 cells are affected by treatment with taxol or OA. As shown in Fig. 6A, after 20 hr of taxol treatment (lane 8) ARE RNA binding activity in cell extracts was substantially reduced relative to untreated extract levels, and no ARE RNA binding activity was detected in extracts after 32 hr (lane 9) of taxol treatment. In extracts of cells treated with OA for 20 hr (Fig. 6B, lane 8), ARE RNA binding activity also was lower than the activity in untreated extracts, while RNA binding activity was not detected in extracts of cells treated with OA for 32 hr (Fig. 6B, lane 9). The temporal correlation between decreased *bcl-2* mRNA levels (Fig. 1) and decreased ARE binding activity in drug treated cells (Fig. 6) suggests HL-60 cells contain stabilizing proteins

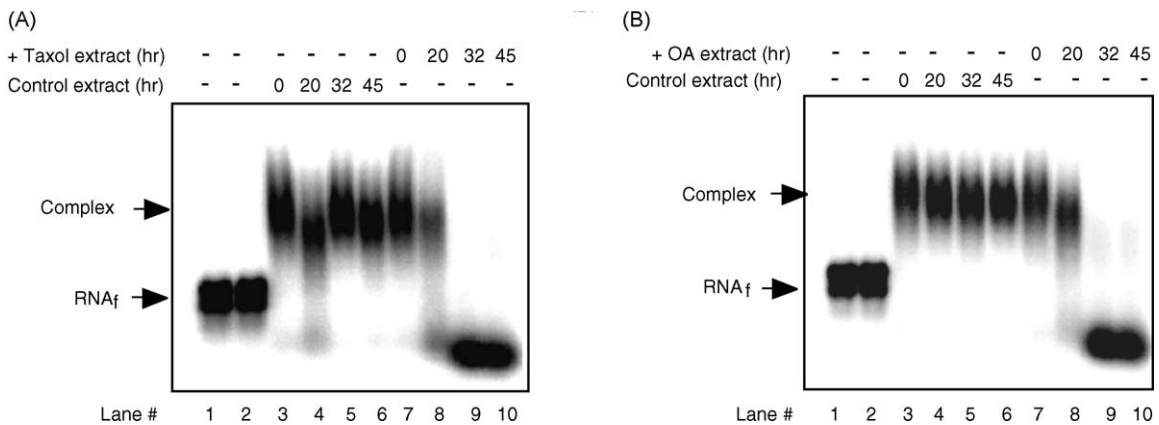

Fig. 6. ARE RNA binding assays of taxol- and OA-treated HL-60 cell extracts. ^{32}P-labeled ARE 1-A transcripts were incubated with cell extracts from untreated cells (lanes 3–6) or (A) taxol-treated cells (lanes 7–10) or (B) OA-treated cells (lanes 7–10). Cells were treated with drugs for the indicated times. Protein–RNA complexes were separated from free RNA (RNA_f) by electrophoresis in 1% agarose gels.

that are progressively inactivated with continuing taxol and OA treatment, potentially leaving *bcl-2* mRNA susceptible to cleavage by endogenous nucleases.

3.5. HuR is not detected in HL-60 cell extract–ARE RNA complexes

One of the best characterized ARE binding proteins is the ubiquitously expressed HuR protein [24], which has been reported to regulate the stability of a number of mRNAs including VEGF [30], p21 [31], cyclins A and B1 [32] and TNF-α [33]. Fan and Steitz [34] found that HuR stabilizes mRNAs containing both Class I and Class II AREs [35]. Myer *et al.* [36] earlier observed that HuR binds weakly to the minimal destabilizing nonamer sequence described by Zubiaga *et al.* [28] (UUAUUUAUU), but binds strongly to $(AUUU)_4A$ and $(AUGU)_4A$ oligonucleotides. The presence of the sequence $(AUUU)_3A$ (which contains the above nonamer sequence) in *bcl-2* ARE 1 suggests HuR may be one of the proteins that binds to *bcl-2* ARE I.

To determine if HuR is present in the protein–RNA complexes formed with HL-60 cell extracts, gel mobility supershift assays with HuR protein and anti-HuR antibody were performed. As shown in Fig. 7A, incubation of purified GST-HuR protein with ARE 1 RNA produced a shift in RNA mobility (lane 2). As expected, the mobility of

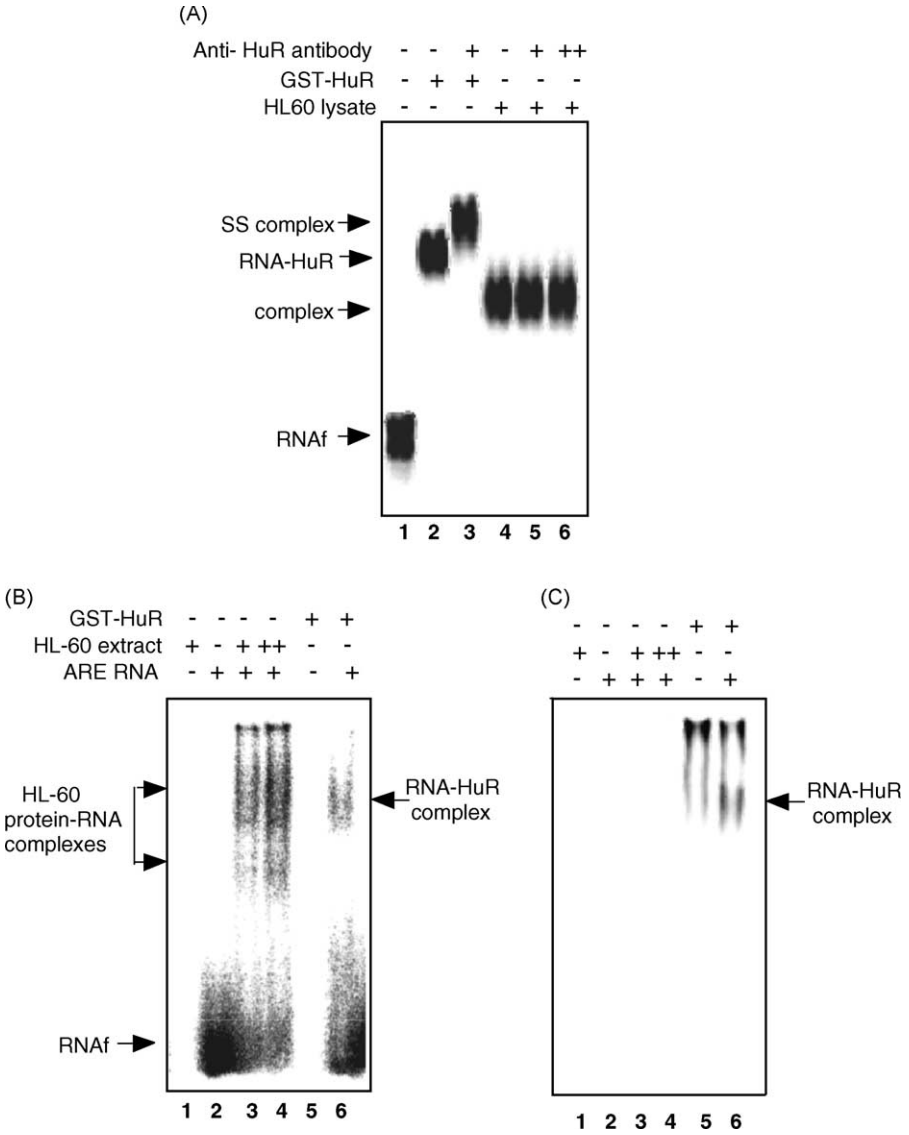

Fig. 7. Assays for the interaction of ARE RNA with HuR. (A) Antibody supershift assay: ^{32}P-labeled ARE 1-A RNA was incubated with GST-HuR (lanes 2 and 3) or with untreated HL-60 cell extracts (lanes 4–6). To test for the presence of HuR in extract protein–RNA complexes, monoclonal anti-HuR antibody was added to the binding reactions in lanes 3, 5 and 6. Samples were analyzed by agarose gel electrophoresis as in Fig. 5. The symbol '+' indicates addition of 20 μg/mL anti-HuR antibody and '++' indicates addition of 40 μg/mL anti-HuR antibody. SS-complex indicates antibody supershifted complexes. (B, C) Gel retardation/Western blot assay. ^{32}P-labeled ARE 1-A RNA was incubated with cell extracts (lanes 3 and 4) or recombinant GST-HuR (lane 6) and then treated with RNAse T1. Protein–RNA complexes were separated on a native 6% polyacrylamide gel. After exposure to a phosphor-image plate (B), proteins in the gel were transferred to nitrocellulose for Western blot analysis with anti-HuR antibody (C). Lane 1, HL-60 extract alone; lane 2, RNA alone; lane 3, 3.7 μg HL-60 extract protein plus RNA; lane 4, 7.5 μg HL-60 extract plus RNA; lane 5, GST-HuR protein alone; lane 6, GST-HuR protein plus RNA.

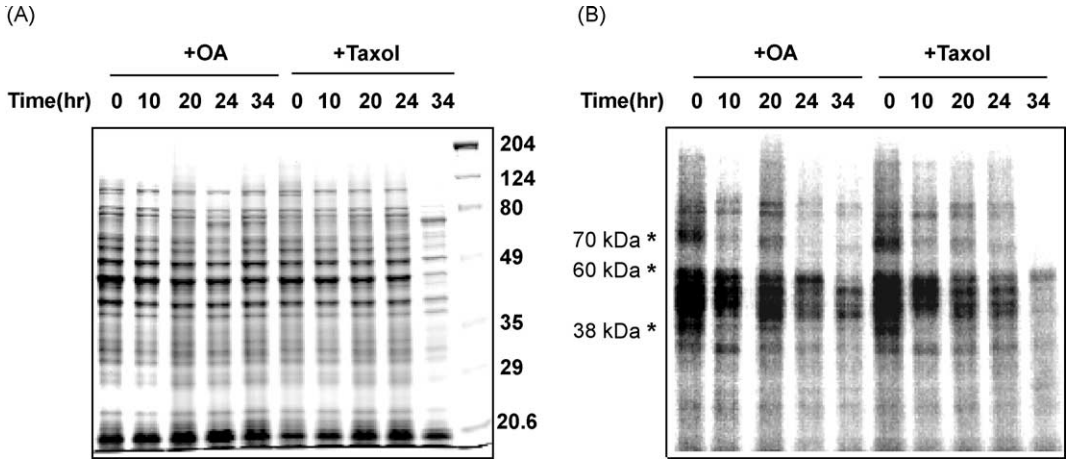

Fig. 8. UV cross-linking assays of HL-60 cell extracts. Total cell extracts from HL-60 cells treated with taxol or OA for 0–34 hr were incubated with ^{32}P-ARE 1 RNA and exposed to UV light (254 nm) for 30 min. Complexes were then digested with RNase A and T1 and separated by SDS–PAGE. Gels were stained with Coomassie Blue and then dried and analyzed for the presence of ^{32}P-RNA by phosphorimaging. Asterisk (*) indicates ~38, ~60 and ~70 kDa proteins cross-linked to RNA. Panels (A) and (B) are Coomassie Blue and phosphorimaging profiles of the gel, respectively.

the GST-HuR–RNA complex was supershifted when the complex was incubated with anti-HuR antibody (lane 3). However, when anti-HuR antibody was incubated with cell extract protein–RNA complexes (lanes 5 and 6) no supershift was observed, and the intensity of the shifted band was not diminished. This result suggests that HuR is not part of the protein–RNA complexes formed with HL-60 cell lysates. However, association of other proteins with HuR in the complex may mask its accessibility to anti-HuR antibody. To examine this possibility, a combined gel shift assay and Western blot was performed to probe for HuR in cell extract–RNA complexes. ARE 1-A RNA was incubated with HL-60 extracts or with GST-HuR protein. The protein–RNA complexes were digested with RNAse T_1 and separated from unbound RNA on a native polyacrylamide gel. The gel was then blotted onto nitrocellulose and probed with anti-HuR antibody. The phosphorimage of the gel (Fig. 7B) demonstrated that incubation of ARE RNA with cell extracts (lanes 3 and 4) or GST-HuR (lane 6) produced RNAse protected ^{32}P-RNA–protein complexes that were resolved on the native gel. However, only the GST-HuR–RNA complex (lane 6) was detected by the anti-HuR antibody in the Western blot analysis (Fig. 7C) of the same gel. Thus, both supershift assays and gel shift/Western blot assays indicate that HuR is not present in the protein–RNA complexes formed with HL-60 extracts.

3.6. Estimation of the number of ARE 1 binding proteins

To determine the size and number of *bcl-2* ARE 1 binding proteins present in HL-60 cell extracts, UV cross-linking assays were performed. Cell extracts were incubated with ^{32}P-ARE-1-A RNA and then exposed to UV light to induce protein–RNA cross-linking. Following RNase digestion of the protein–RNA complexes, proteins were separated by SDS–PAGE. The gels were stained with Coomassie Blue (Fig. 8A) and the presence of ^{32}P-labeled protein was detected by phosphorimaging. As shown in Fig. 8B, approximately eight proteins or polypeptide fragments, ranging in size from 100 to 32 kDa, were cross-linked to ^{32}P-labeled ARE 1 RNA. Interestingly, UV-induced RNA cross-linking to ~70 and ~38 kDa proteins was notably reduced in extracts of cells treated with taxol for 10 hr or cells treated with OA for 20 hr. In addition, cross-linking to 45–60 kDa proteins progressively decreased with 10–34 hr of either OA or taxol treatment (Fig. 8B). To determine if cross-linked proteins bind specifically to *bcl-2* ARE 1 RNA, competition assays were

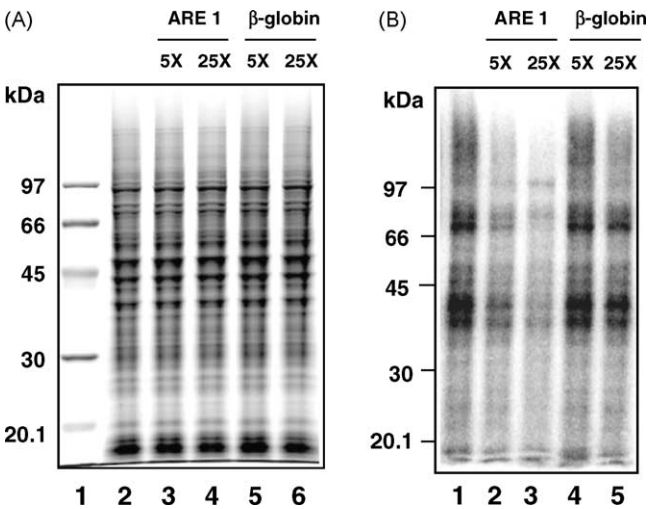

Fig. 9. Specificity of UV cross-linking of HL-60 cell extracts. Total cell extracts from HL-60 cells were incubated with ^{32}P-ARE-1-A RNA in the absence (lane 1) or the presence of 5- or 25-fold excesses of unlabeled homologous *bcl-2* ARE 1-A RNA or heterologous *β-globin* RNA. Samples were exposed to UV light for 30 min and then digested with RNase A and T1 and separated by SDS–PAGE. Gels were analyzed as in Fig. 8. Panels (A) and (B) are Coomassie Blue and phosphorimaging profiles of the gel, respectively.

performed. Addition of a 5× or 25× excess concentration of unlabeled *β-globin* mRNA did not appreciably reduce cross-linking of the 38–70 kDa proteins to ^{32}P-ARE RNA, while addition of homologous ARE RNA did reduce cross-linking (Fig. 9). Thus the major crosslinking proteins bind specifically to *bcl-2* ARE 1 RNA.

4. Discussion

We have found that taxol treatment downregulates and destabilizes *bcl-2* mRNA in HL-60 cells. The time course of destabilization of *bcl-2* mRNA with taxol was similar to that observed with OA treatment. Importantly, *bcl-2* mRNA downregulation precedes the early events of apoptosis induced by taxol or OA, suggesting that decreases in *bcl-2* mRNA are not a result of the induction of apoptosis in these cells. As described below, our findings collectively support the conclusion that both taxol- and OA-induced *bcl-2* mRNA downregulation involves inactivation of *bcl-2* mRNA stabilizing factors.

Studies by Schiavone *et al.* [15] demonstrated that a 400 nucleotide segment of the 3′-UTR of *bcl-2* mRNA contains an ARE that exhibits intrinsic destabilizing activity. In this report, we show that an internal 137 nucleotide sequence which contains two AUUUA pentamers and an overlapping pentamer sequence $(AUUU)_3A$, has the same destabilizing effect on *β-globin* mRNA as the full 400 nucleotide sequence. Gel mobility shift assays demonstrated that proteins in HL-60 cell extracts bind specifically to ARE 1-A RNA. In contrast, extracts of HL-60 cells treated with taxol or OA for 32 hr did not exhibit ARE 1-A RNA binding activity. The loss of ARE RNA binding activity in cell extracts was temporally correlated with decreased *bcl-2* mRNA steady state levels. This finding, coupled with the observed decrease in *bcl-2* mRNA half-life following taxol or OA treatment, suggests that HL-60 cells contain *bcl-2* mRNA stabilizing factors that are inactivated by OA or taxol treatment. Consistent with this conclusion, we found that *bcl-2* ARE mRNA decayed faster in taxol- and OA-treated cell extracts than in extracts of untreated HL-60 cells.

UV cross-linking assays further demonstrated that approximately eight proteins or polypeptide fragments in HL-60 cell extracts interact with ARE 1 RNA *in vitro*. Interestingly, the efficiency of cross-linking of ARE RNA to two proteins (i.e. ∼38 and ∼70 kDa proteins) was greatly diminished within 10–20 hr following addition of taxol or OA to HL-60 cells, while cross-linking of four other proteins of 45–60 kDa sizes progressively decreased with taxol or OA treatment from 10 to 34 hr. The decreases in protein–ARE RNA cross-linking were temporally correlated with the downregulation of *bcl-2* mRNA by taxol or OA, suggesting that the ARE-binding proteins play a role in regulating *bcl-2* mRNA stability. Taken together, these findings demonstrate that taxol treatment modulates the activities of the same *bcl-2* ARE-binding proteins as OA treatment, suggesting that the two apoptotic stimuli induce *bcl-2* mRNA downregulation by similar pathways.

The effects on *bcl-2* ARE-binding proteins produced by taxol and OA in HL-60 cells appears to be different from the effects of UV-C irradiation observed in Jurkat cells. Donnini *et al.* [18] found that during UV-C-induced apoptosis of Jurkat cells, decreases in *bcl-2* mRNA levels were accompanied by an increase in ARE-binding proteins in cytoplasmic extracts. Subsequently, it was found that UV-C treatment induces an increase in the p45 isoform of AUF1 in Jurkat cytoplasmic extracts as well as an increase in UV-induced cross-linking of p45 to ARE riboprobes [19]. Collectively, these studies suggest that induction of apoptosis by UV-C irradiation induces the activity of destabilizing proteins, including one or more isoforms of AUF1. In contrast, taxol and OA appear to decrease the activity of *bcl-2* mRNA stabilizing proteins in HL-60 cells. Interestingly, although the mechanism of *bcl-2* mRNA destabilization appears to be different in the two cases, they both involve protein interactions with *bcl-2* ARE 1.

Although it is not yet clear how the two *bcl-2* mRNA destabilization pathways are related, it is likely that observed differences in responses to extracellular stimuli are related to differences in the cellular components affected by UV-C irradiation versus taxol and OA, as well as to inherent differences between Jurkat and HL-60 cells. For example, since *bcl-2* mRNA levels are elevated in HL-60 cells relative to normal B cells and Jurkat cells [20], specific proteins may be overexpressed or activated in HL-60 cells that stabilize *bcl-2* mRNA, presumably through an ARE-dependent mechanism. In other cells, *bcl-2* mRNA may be intrinsically unstable but exhibit increased stability in the presence of specific stimuli. For example, TPA treatment of Jurkat cells has been found to increase the stability of *bcl-2* mRNA [15]. Overall, it is clear from the results reported here and the earlier studies [18,19] that multiple proteins interact with the *bcl-2* ARE and that some proteins (e.g. the 38 and 70 kDa RNA cross-linking proteins) may perform stabilizing functions while others, such as AUF1, may contribute to the destabilization of *bcl-2* mRNA.

The studies described herein suggest a novel strategy for decreasing *bcl-2* protein and inducing apoptosis in cancer cells. We have shown that taxol and OA can decrease *bcl-2* mRNA levels by inducing *bcl-2* mRNA destabilization. Because of the pivotal role of the *bcl-2* oncogene in the development of certain cancers, drug-induced destabilization of *bcl-2* mRNA may be a useful pharmacological approach for reversing the malignant phenotype of B-cell lymphomas and certain solid tumors. Our ongoing experiments are aimed at identifying the *trans*-acting protein(s) involved in *bcl-2* mRNA stabilization and the possible mechanisms by which anti-cancer drugs downregulate the binding of these proteins to *bcl-2* mRNA.

Acknowledgments

The authors thank David Priest and Chris Davies for helpful discussions. We thank Tanvir Mahtab for assistance in preparing pBBB-ARE$^{bcl\text{-}2}$ plasmids and Fredilyn Lipata for excellent technical assistance. We are also grateful to A.-B. Shyu for providing plasmids pBBB4 and pBBB-ARE$^{c\text{-}fos}$ and H. Furneaux for providing pGEX-HuR. We thank the MUSC Biotechnology Resource Laboratory for expert DNA sequence analysis. This work was supported in part by development funds awarded to the Hollings Cancer Center by the U.S. Department of Defense and by Public Health Service Grant CA 87553 (to E.K.S.) from the National Cancer Institute.

References

[1] Vaux DL, Cory S, Adams JM. *Bcl-2* gene promotes haemopoietic cell survival and cooperates with c-*myc* to immortalize pre-B cells. Nature 1988;335:440–2.

[2] Cleary ML, Smith SD, Sklar J. Cloning and structural analysis of cDNAs for *bcl-2* and a hybrid *bcl-2*/immunoglobulin transcript resulting from the t(14;18) translocation. Cell 1986;47:19–28.

[3] Reed JC. Bcl-2 family proteins: strategies for overcoming chemoresistance in cancer. Adv Pharmacol 1997a;41:501–32.

[4] Campos L, Rouault J-P, Sabido O, Oriol P, Roubi N, Vasselon C, Archimbaud E, Magaud J-P, Guyotat D. High expression of *bcl-2* protein in acute myeloid leukemia cells is associated with poor response to chemotherapy. Blood 1993;81:3091–6.

[5] Reed JC. Bcl-2 family proteins: regulators of apoptosis and chemoresistance in hematologic malignancies. Sem Hemat 1997b;34:9–19.

[6] Gao G, Dou Q-P. G_1 phase-dependent expression of *Bcl-2* mRNA and protein correlates with chemoresistance of human cancer cells. Mol Pharmacol 2000;58:1001–10.

[7] Liu Y, Priest DG. Enhancement of *Bcl-2* mRNA degradation by taxol and other anticancer drugs that induce apoptotic cell death. Cell Pharmacol 1996;3:405–8.

[8] Riordan FS, Foroni L, Hoffbrand V, Mehta AB, Wickremasinghe RG. Okadaic acid-induced apoptosis of HL-60 leukemia cells is preceded by destabilization of *bcl-2* mRNA and downregulation of bcl-2 protein. FEBS Lett 1998;435:195–8.

[9] Shaw G, Kamen R. A conserved AU sequence from the untranslated region of GM-CSF mRNA mediates selective mRNA degradation. Cell 1986;46:659–67.

[10] Stoecklin G, Hahn S, Moroni C. Functional hierarchy of AUUUA motifs in mediating rapid interleukin-3 mRNA decay. J Biol Chem 1994;269:28591–7.

[11] Treisman R. Transient accumulation of c-*fos* RNA following serum stimulation requires a conserved 5′ element and c-*fos* 3′ sequences. Cell 1985;42:889–902.

[12] Schiavi SC, Belasco JG, Greenberg ME. Regulation of proto-oncogene mRNA stability. Biochim Biophys Acta 1992;1114:95–106.

[13] Chen C-YA, Shyu A-B. AU-rich elements: characterization and importance in mRNA degradation. Trends Biochem Sci 1995;20:465–70.

[14] Xu N, Chen CY, Shyu AB. Modulation of the fate of cytoplasmic mRNA by AU-rich elements: key sequence features controlling mRNA deadenylation and decay. Mol Cell Biol 1997;17:4611–21.

[15] Schiavone N, Rosini P, Quattrone A, Donnini M, Lapucci A, Citti L, Bevilacqua A, Nicolin A, Capaccioli S. A conserved AU-rich element in the 3′ untranslated region of *bcl-2* mRNA is endowed with a destabilizing function that is involved in *bcl-2* down-regulation during apoptosis. FASEB J 2000;14:174–84.

[16] Shyu A-B, Greenberg ME, Belasco JG. The c-*fos* transcript is targeted for rapid decay by two distinct mRNA degradation pathways. Genes Dev 1989;3:60–72.

[17] Wisdom R, Lee W. The protein-coding region of c-*myc* mRNA contains a sequence that specifies rapid mRNA turnover and induction by protein synthesis inhibitors. Genes Dev 1991;5:232–43.

[18] Donnini N, Lapucci A, Papucci L, Witort E, Tempestini A, Brewer G, Bevilacqua M, Nicolin A, Capaccioli S, Schiavone N. Apoptosis is associated with modifications of *bcl-2* mRNA AU-binding proteins. Biochem Biophys Res Commun 2001;287:1063–9.

[19] Lapucci A, Donnini M, Papucci L, Witort E, Tempestini A, Bevilacqua M, Nicolin A, Brewer G, Schiavone N. Capaccioli, AUF1 is a *bcl-2* A + U-rich element-binding protein involved in *bcl-2* mRNA destabilization during apoptosis. J Biol Chem 2002;277:16139–46.

[20] Steube KG, Jadau A, Teepe D, Drexler HG. Expression of *bcl-2* mRNA and protein in leukemia–lymphoma cell lines. Leukemia 1995; 9:1841–6.

[21] Tsujimoto Y, Croce CM. Analysis of the structure, transcripts, and protein products of *bcl-2*, the gene involved in human follicular lymphoma. Proc Natl Acad Sci USA 1986;83:5214–8.

[22] Chen C-Y, Chen T-M, Shyu A-B. Interplay of two functionally and structurally distinct domains of the c-*fos* AU-rich element specifies its mRNA-destabilizing function. Mol Cell Biol 1994;14:416–26.

[23] Ford LP, Wilusz J. An *in vitro* system using HeLa cytoplasmic extracts that reproduces regulated mRNA stability. Methods 1999;17:21–7.

[24] Ma WJ, Cheng S, Campbell C, Wright A, Furneaux H. Cloning and characterization of HuR, a ubiquitously expressed elav-like protein. J Biol Chem 1996;271:8144–51.

[25] Koopman G, Reutelingsperger CP, Kuijten GA, Keehnen RM, Pals ST, van Oers MH. Annexin V for flow cytometric detection of phosphatidylserine expression on B cells undergoing apoptosis. Blood 1994; 84:1415–20.

[26] Altschul SF, Madden TL, Schaffer AA, Zhang Z, Miller W, Lipman DJ. Gapped BLAST and PSI-BLAST: a new generation of protein database search programs. Nucleic Acids Res 1997;25:3389–402.

[27] Tholanikunnel BG, Malbon CC. A 20-nucleotide (A + U)-rich element of β_2-adrenergic receptor (β_2AR) mRNA mediates binding to β_2AR-binding protein and is obligate for agonist-induced destabilization of receptor mRNA. J Biol Chem 1997;272:11471–8.

[28] Zubiaga AM, Belasco JG, Greenberg ME. The nonamer UUAUUUAUU is the key AU-rich sequence motif that mediates mRNA degradation. Mol Cell Biol 1995;15:2219–30.

[29] Chen C-Y, Shyu A-B. Selective degradation of early-response-gene mRNAs: functional analyses of sequence features of the AU-rich elements. Mol Cell Biol 1995;14:8471–82.

[30] Levy NS, Chung S, Furneaux H, Levy AP. Hypoxic stabilization of vascular endothelial growth factor mRNA by the RNA-binding protein HuR. J Biol Chem 1998;173:6417–23.

[31] Wang W, Furneaux H, Cheng H, Caldwell MC, Hutter D, Liu Y, Holbrook N, Gorospe M. HuR regulates p21 mRNA stabilization by UV light. Mol Cell Biol 2000a;20:760–9.

[32] Wang W, Caldwell MC, Lin S, Furneaux H, Gorospe M. HuR regulates cyclin A and cyclin B1 mRNA stability during cell proliferation. EMBO J 2000b;19:1–12.

[33] Dean JLE, Wait R, Mahtani KR, Sully G, Clark AR, Saklatvala J. The 3′ untranslated region of tumor necrosis factor alpha mRNA is a target of the mRNA-stabilizing factor HuR. Mol Cell Biol 2001;21:721–30.

[34] Fan XC, Steitz JA. Overexpression of HuR, a nuclear-cytoplasmic shuttling protein, increases the *in vivo* stability of ARE-containing mRNAs. EMBO J 1998;17:3448–60.

[35] Shyu A-B, Belasco JG, Greenberg ME. Two distinct destabilizing elements in the c-*fos* message trigger deadenylation as a first step in rapid mRNA decay. Genes Dev 1991;5:221–31.

[36] Myer VE, Fan XC, Steitz JA. Identification of HuR as a protein implicated in AUUUA-mediated mRNA decay. EMBO J 1997;16: 2130–9.